830-H-15 NAS1.60:1691

OCT 14 1980

NASA Technical Paper 1691

COMPLETED

ORIGINAL

Long-Time Creep Behavior of the Tantalum Alloy Astar 811C

William D. Klopp, Robert H. Titran,
and Keith D. Sheffler

SEPTEMBER 1980

NASA

21

NASA Technical Paper 1691

Long-Time Creep Behavior of the Tantalum Alloy Astar 811C

William D. Klopp and Robert H. Titran
Lewis Research Center
Cleveland, Ohio

Keith D. Sheffler
Pratt & Whitney Aircraft
East Hartford, Connecticut

National Aeronautics
and Space Administration

**Scientific and Technical
Information Branch**

1980

A

Summary

The long-time, high-vacuum creep behavior of Astar 811C (Ta-8W-1Re-0.7Hf-0.025C) has been studied as a function of stress, temperature, and grain size. Primary creep strain was related to time by the Garofalo exponential function, and a second exponential term was developed to describe the tertiary portion of the creep curve. No significant periods of secondary (linear) creep were observed. The creep curves were well expressed by a relation that includes only terms for primary and tertiary creep:

$$\epsilon = \epsilon_0 + \epsilon_p\ (1 - e^{-rt}) + K(e^{st} - 1)$$

The initial primary and tertiary creep rates $\epsilon_p r$ and Ks, obtained by differentiating the respective terms from the strain-time relation, can be related to temperature by using a dual activation energy to account for lattice and dislocation core diffusion. The term $\epsilon_p r$ is expressed as an exponential function of stress, and Ks can be related to stress by the sinh function. At small grain sizes, Ks is proportional to the inverse square of grain size. The strain parameters ϵ_p and K were determined as power functions of the applied stress. The overall relation for the initial tertiary creep rate Ks is

$$Ks = A\left[\left(\sinh\frac{\alpha\sigma}{E}\right)^{n_1} + \left(\frac{f}{d^2}\right)\left(\sinh\frac{\alpha\sigma}{E}\right)^{n_2}\right] \times \left(e^{-Q_1/RT} + c\,e^{-Q_2/RT}\right)$$

where A is the proportionality constant, α is the stress factor, σ is the stress, E is Young's modulus, f is the grain-size factor, d is the grain size, n is the stress exponent, Q is the activation energy, R is the gas constant, T is the temperature, and c is the temperature factor.

Similar relations were developed for the initial primary creep rate $\epsilon_p r$, the minimum creep rate ϵ_m and the time to 1 percent strain.

Introduction

Previous studies on the long-time creep behavior of Ta-10W (ref. 1), T-111 (ref. 2), T-222 (ref. 3), and niobium alloys (refs. 4 to 7) have shown that they sometimes exhibit only primary (decelerating) and/or tertiary (accelerating) creep. Often only tertiary creep is observed for these materials at high temperatures. Secondary (linear) creep, which is an integral part of most current creep theories, is frequently only a transition between the primary and tertiary creep stages. Creep curves for these materials can be expressed by a series of polynomials with time exponents ranging from 1/2 to 5/2 (refs. 1, 3, and 7). Although these and other similar relations are useful in empirically describing creep curves (ref. 8), the use of multiple terms unduly increases the complexity of analysis.

Wilshire and coworkers (refs. 9 and 10) have also developed a relation for describing creep curves exhibiting primary, secondary, and tertiary creep stages. However, the term describing tertiary creep requires as input the time for onset of tertiary creep, which is difficult to predict.

Strong grain-size effects were also noted in these studies on niobium and tantalum alloys (refs. 1, 3, and 7), with the coarse-grained materials being much stronger than the fine-grained materials. Such behavior in alloys is well known (ref. 11), although the functional form of the relation between creep rate and grain size has not yet been clearly defined.

The primary purpose of the present study was to develop a relation for correlating and predicting strain-time curves during long-time creep for Astar 811C over the temperature range 800° to 1700° C as a function of stress, temperature, and grain size. A secondary purpose was to compare the long-time creep strength of Astar 811C with that of other tantalum alloys.

Steven M. Sidik and Raymond W. Palmer of the Lewis Research Center designed the nonlinear regression programs for this study.

Symbols

A	proportionality constant, various dimensions
b	grain-size exponent for tertiary creep strain parameter, dimensionless
c	temperature factor, dimensionless
d	grain size, cm
d_0	initial grain size, cm
E	Young's modulus, MPa
f	grain-size factor, cm^2

K	tertiary creep strain parameter, dimensionless
m	stress exponent for primary creep strain, dimensionless
n	stress exponent, dimensionless
Q	activation energy, kJ/g mol
R	gas constant, kJ/(g mol) (deg)
r	primary creep rate parameter, sec^{-1}
s	tertiary creep rate parameter, sec^{-1}
T	temperature, K
t	time, sec
t_{1pct}	time to 1 percent strain, sec
α	stress factor, dimensionless
β	stress factor, dimensionless
ϵ	creep strain, dimensionless
ϵ_p	total primary creep strain, dimensionless
ϵ_0	initial creep strain, dimensionless
$\dot{\epsilon}$	creep rate, sec^{-1}
$\dot{\epsilon}_m$	minimum creep rate, sec^{-1}
σ	stress, MPa

Experimental Procedure

Three lots of material—designated as lots, A, B, and C—were used in this study. These materials were procured commercially and had been cold-rolled 90 percent to 0.076-cm-thick sheet after the last in-process anneal. Chemical analyses of the starting materials are given in table I.

This study included creep specimens of two sizes, each tested at a different laboratory. Creep specimens labeled "N" were tested at the NASA Lewis Research Center; those labeled "S" were tested at the TRW-Colwell Research Laboratory (under contract NAS3-15554). The reduced gage sections were 2.54 cm by 0.635 cm for the N specimens and 5.08 cm by 1.27 cm for the S specimens. All specimens were machined with the longitudinal direction of the reduced section parallel to the final rolling direction.

The specimens were annealed before creep testing, generally for 1 hr at 1649° C (average grain size, 1.7 μm), or for 0.5 hr at 1982° C (average grain size, 9.4 μm). Selected other treatments, ranging from 0.25 to 100 hr at 1538° to 2205° C, were designed to give a range of grain sizes. The N specimens were annealed separately in a high-vacuum, titanium-sputter-ion-pumped furnace at pressures of less than 10^{-9} Pa. The S specimens were annealed in situ in the high-vacuum, titanium-sputter-ion-pumped creep furnaces just before the creep tests.

The high-vacuum, titanium-sputter-ion-pumped creep furnaces used at NASA and at TRW are similar and have been described previously (refs. 5 and 12). Complete thermal equilibrium of specimens was insured by a 2-hr hold at the test temperature before the load was applied. Pressure was always below 10^{-10} Pa during the tests and generally fell into the 10^{-12}-Pa range as testing proceeded. For the N specimens temperatures were measured by Pt/Pt-13%Rh thermocouples. For the S specimens an optical pyrometer with a precision of ±1 degree C was initially calibrated against a thermocouple reading and was then used as the prime temperature reference throughout each test.

Temperature control for all tests was within ±3 degrees C. Specimen extensions were determined with optical extensometers that measured the distance between scribed reference marks to an accuracy of ±1 μm. Strains on loading were measured and are incorporated in the total creep strains. Creep testing was usually terminated after total creep strains of 1 to 3 percent were achieved. However, some tests were terminated before

TABLE I. - ANALYSES OF MATERIALS

Lot	Element						
	W	Re	Hf	C	O	N	H
	Analyzed composition[a], wt %						
A	7.52±0.33(8)	1.02±0.11(7)	0.87±0.25(8)	0.0250±0.0031(10)	0.0013±0.0007(14)	0.0018±0.0012(9)	0.0003±0.0002(8)
B	8.10±0.35(5)	1.18±0.04(5)	0.91±0.13(5)	0.0244±0.0023(6)	0.0032±0.0014(5)	0.0024±0.0012(6)	0.0003±0.0002(5)
C	7.74±0.05(2)	1.12±0.01(2)	1.22±0.04(2)	0.0139±0.0079(9)	0.0015±0.0001(2)	0.0008±0.0000(2)	0.0002±0.0000(2)

[a]Mean compositions and standard deviations from means are given. Number in parentheses is number of analyses. Both ingot and sheet analyses are averaged for lots A and B; only sheet analyses are available for lot C.

1 percent strain was achieved, and a few were allowed to reach strains up to 15 percent. No significant differences in creep behavior were observed between the N and S specimens.

Post-test examinations for both the N and S specimens included selected chemical analyses for possible oxygen or nitrogen contamination and/or carbon loss during creep testing. Metallographic examinations were conducted to determine final grain sizes by the boundary-intercept method and to observe carbide morphologies. Scanning electron microscopy was used for detailed studies of the microstructure. X-ray emission analyses also were conducted to identify bromine-extracted particles from selected specimens.

For data correlation all stresses were divided by Young's modulus (ref. 13). Data on moduli for Astar 811C were obtained from reference 14.

Results and Discussion

Shapes of Creep Curves

Typical long-time creep curves for Astar 811C are shown in figures 1 to 3. At high stresses (i.e., above about 1.5×10^{-3} σ/E) only primary (decelerating) creep was observed, as shown in figure 1. However, at intermediate stresses of about 1.0×10^{-3} to 1.5×10^{-3} σ/E both primary and tertiary (accelerating) creep were observed, as shown in figure 2. At stresses below 1.0×10^{-3} σ/E generally only tertiary creep was observed. Typical curves of this latter type are shown in figure 3.

Creep data from those tests exhibiting only primary creep were fitted by nonlinear regression to the primary creep term of the relation suggested by Garofalo (ref. 15):

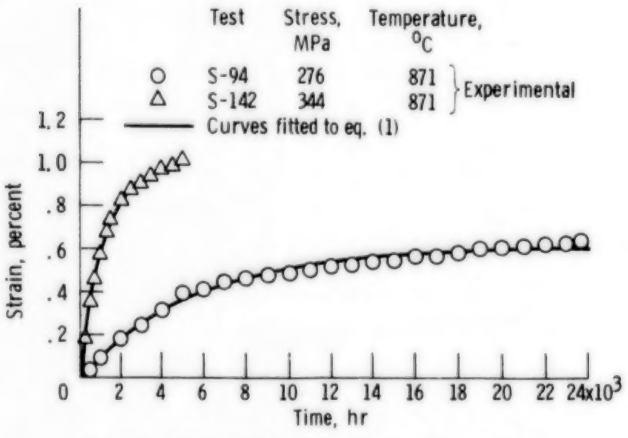

Figure 1. - Typical high-stress creep curves showing only primary creep of Astar 811C.

$$\epsilon = \epsilon_0 + \epsilon_p(1 - e^{-rt}) \tag{1}$$

where ϵ is strain at time t, ϵ_0 is strain on loading (or strain deviation at zero time), ϵ_p is total primary strain, and r is the primary creep rate parameter.

A few tests exhibited secondary creep after initial primary creep. For these tests the test times were probably insufficient to allow tertiary creep to become apparent. These curves were fitted to the complete primary-plus-secondary Garofalo relation:

$$\epsilon = \epsilon_o + \epsilon_p(1 - e^{-rt}) + \dot{\epsilon}_m t \tag{2}$$

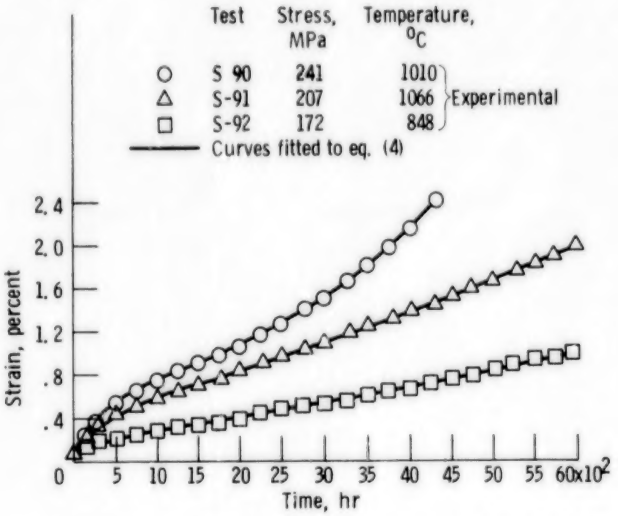

Figure 2. - Typical intermediate-stress creep curves showing both primary and tertiary creep of Astar 811C.

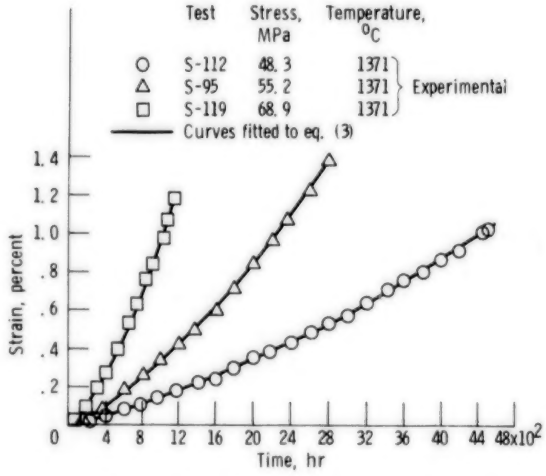

Figure 3. - Typical low-stress creep curves showing only tertiary creep of Astar 811C.

TABLE II. - TEST CONDITIONS AND CREEP RESULTS

Lot	Test	Annealing conditions		Test temperature, °C	Stress, MPa	Ratio of stress to Young's modulus, σ/E	Primary creep strain parameter, ϵ_p	Primary creep rate parameter, r, sec^{-1}	Minimum creep rate, ϵ_m, sec^{-1}	Tertiary creep strain parameter, K	Tertiary creep rate parameter, s, sec^{-1}	Time to 1 percent strain, hr	Grain diameter, d, μm	Test duration	
		Time, hr	Temperature, °C											Time, hr	Strain, percent
A	N-4	1	1538	1316	82.7	5.04×10^{-4}	----------	----------	190×10^{-10}	1.06×10^{-2}	233×10^{-8}	77.9	15	188	[a]4.10
	N-2	1	1649	1316	55.2	3.36	----------	----------	19.3	.951	18.1	1 040	20	1 843	[b]2.32
	N-1	↓	↓	↓	82.7	5.04	----------	----------	53.6	.842	67.3	297	----	406	1.51
	N-5				82.7	5.04	----------	----------	60.2	.845	70.0	283	20	361	1.33
	S-75				103	6.30	----------	----------	153	.836	150	143	21	162	1.20
	N-6		1760		82.7	5.04	----------	----------	37.7	1.21	29.0	557	44	1 440	[a]4.27
	S-70	.25	1938	1149	138	8.25	0.130×10^{-2}	14.4×10^{-6}	6.34	----------	----------	--------	52	978	.34
	S-71	.15	1982	1149	138	8.25	.075	4.50	6.83	----------	----------	--------	55	762	.32
	N-7	1	1871	1316	82.7	5.04	----------	----------	24.6	1.25	16.2	1 020	65	1 199	1.15
	S-73	.33	1982	1316	103	6.30	----------	----------	57.8	2.02	25.4	444	67	713	1.86
	N-34	.5	1982	982	193	11.34	.206	.557	.421	----------	----------	--------	-----	1 535	.28
	N-13	↓	↓	1093	110	6.56	----------	----------	----------	----------	----------	--------	-----	2 567	[c].19
	N-38			1093	138	8.20	.098	1.90	.864	----------	----------	--------	-----	10 030	.45
	N-30			1093	193	11.48	.214	6.37	46.4	3.99	11.1	412	-----	479	1.16
	N-26			1204	68.9	4.15	----------	----------	.962	----------	----------	--------	-----	7 851	[d].34
	N-35			1204	110	6.64	----------	----------	5.11	----------	----------	4 920	-----	7 341	[d]1.44
	N-27			1204	138	8.30	----------	----------	23.6	2.73	8.53	897	-----	1 109	1.27
	N-40			1260	68.9	4.18	----------	----------	2.01	1.01	2.06	8 130	-----	8 471	1.04
	N-29			1260	138	8.35	----------	----------	87.4	----------	----------	281	-----	358	[d]1.27
	N-33			1260	138	8.35	----------	----------	78.7	3.12	22.8	311	-----	407	1.32
	N-21			1316	41.4	2.52	----------	----------	1.21	1.48	.898	--------	-----	10 042	.58
	N-25			↓	55.2	3.36	----------	----------	2.62	.688	2.99	7 700	-----	8 180	1.06
	N-28				68.9	4.20	----------	----------	10.5	2.05	4.31	2 280	-----	2 925	1.32
	N-36				110	6.72	----------	----------	112	1.76	54.2	220	-----	313	1.60
	N-23			1371	27.6	1.69	----------	----------	.895	.092	7.09	9 430	-----	10 056	1.27
	N-18			1371	68.9	4.24	----------	----------	32.9	1.87	16.9	683	121	1 341	2.36
	N-22			1427	27.6	1.71	----------	----------	2.67	.167	12.4	--------	-----	4 580	[e]1.25
	N-20			↓	41.4	2.56	----------	----------	8.93	.548	18.1	--------	125	1 470	.93
	N-10				55.2	3.42	----------	----------	59.0	1.23	51.4	316	-----	524	2.03
	N-14				68.9	4.27	----------	----------	195	1.33	113	117	63	263	2.75
	N-15			↓	68.9	4.27	----------	----------	146	1.41	100	138	63	289	2.63
	N-19			1482	27.6	1.72	----------	----------	14.2	.285	42.8	960	147	1 437	2.30
	N-31			1482	41.4	2.59	----------	----------	74.3	2.04	32.1	338	-----	361	1.11
	N-32			1538	13.8	.870	----------	----------	8.07	.395	18.8	--------	-----	838	[f].50
	N-37	↓	↓	1538	13.8	.870	----------	----------	9.92	.182	51.3	--------	-----	514	[f].34

A	N-16	.5	1982	1538	27.6	1.74×10^{-4}	----------	----------	71.2×10^{-10}	0.680×10^{-2}	113×10^{-8}	226	79	315	1.75
	N-24	.5	↓	1538	41.4	2.61	----------	----------	146	.795	187	113	144	166	1.69
	N-11	.5		1538	55.2	3.48	----------	----------	423	1.02	398	44.8	86	144	[a]6.75
	N-8	1		1316	82.7	5.04	----------	----------	20.6	3.22	6.06	1 190	107	1 676	1.46
	S-79	5	1899	↓	103	6.30	----------	----------	49.8	2.93	15.1	545	144	714	1.40
	S-81	24	1799		103	6.30	----------	----------	49.6	2.92	15.3	524	144	667	1.33
	N-43	1	2093		82.7	5.04	----------	----------	19.4	.930	18.0	1 110	246	1 248	1.17
	N-44	1	2205	↓	82.7	5.04	----------	----------	10.8	.801	13.9	1 620	250	2 021	1.41
B	S-142	1	1649	871	344	19.98×10^{-4}	0.96×10^{-2}	0.224×10^{-6}	----------	----------	----------	4 790	18	4 998	1.01
	S-210	↓	↓	982	228	13.36	.373	8.70	2.90×10^{-10}	----------	----------	--------	18	2 206	.60
	S-174			982	248	14.57	.571	4.89	5.17	1.32×10^{-2}	3.70×10^{-8}	2 160	18	4 868	[g]1.92
	S-131			982	276	16.19	.969	1.36	----------	----------	----------	569	17	867	1.15
	S-160			1038	228	13.44	.471	12.8	11.4	----------	----------	1 350	19	2 019	1.29
	S-128			1038	248	14.65	.694	9.90	30.0	----------	----------	287	-----	649	1.39
	S-125			1093	159	9.43	.061	1.96	.764	.773	.970	--------	-----	13 413	[h].74
	S-126			↓	179	10.66	.128	1.31	.496	1.36	2.99	4 380	17	4 627	1.05
	S-118				200	11.89	.231	8.23	12.7	----------	----------	1 640	19	1 655	1.01
	S-134			↓	228	13.52	.426	31.5	87.9	----------	----------	181	18	354	1.55
	S-177			1204	89.6	5.39	----------	----------	21.3	1.06	2.23	8 260	-----	8 877	1.09
	S-143			1204	124	7.47	----------	----------	5.07	.633	9.50	2 800	16	3 650	1.56
	S-136			1204	159	9.54	----------	----------	50.4	1.46	28.0	497	16	501	1.01
	S-204			1316	20.7	1.26	----------	----------	----------	----------	----------	--------	17	2 878	[i].17
	S-195			↓	34.5	2.10	----------	----------	3.46	.449	7.15	--------	16	4 493	[b]1.35
	S-144				55.2	3.36	----------	----------	4.95	.314	16.4	--------	-----	5 541	[b]1.03
	S-135				89.6	5.46	----------	----------	31.9	.456	63.0	516	17	531	1.04
	S-101			↓	103	6.30	----------	----------	73.6	.616	116	233	-----	674	[a]12.18
	S-193			1427	6.89	.427	----------	----------	----------	----------	----------	--------	-----	4 991	[j].93
	S-188			↓	13.8	.855	----------	----------	----------	----------	----------	--------	18	1 076	[j]1.28
	S-147				20.7	1.28	----------	----------	----------	----------	----------	--------	20	1 034	[j]1.76
	S-129			↓	34.5	2.14	----------	----------	----------	----------	----------	--------	19	435	[j]1.76
	S-197			1538	3.45	.217	----------	----------	----------	----------	----------	--------	-----	4 025	[j].62
	S-180			1538	6.89	.435	----------	----------	----------	----------	----------	-- -----	112	1 455	[j]1.55
	S-203	↓	↓	1699	3.45	.221	----------	----------	----------	----------	----------	--------	-----	2 492	[j].13

[a] Portion of curve above 3 percent strain excluded from analysis.

[b] Portion of curve above 1700 hr excluded from analysis because of excessive calculated grain growth.

[c] Curve not analyzed because of erratic behavior.

[d] Curve was linear.

[e] Portion of curve above 3900 hr excluded from analysis because of excessive calculated grain growth.

[f] Portion of curve above 450 hr excluded from analysis because of excessive calculated grain growth.

[g] Portion of curve above 1.44 percent strain excluded from analysis because of erratic behavior.

[h] Portion of curve above 0.24 percent strain excluded from analysis because of erratic behavior.

[i] Insufficient creep data for accurate analysis.

[j] Curve not analyzed because of excessive calculated grain growth.

TABLE II. - Concluded.

Lot	Test	Annealing conditions		Test temperature, °C	Stress, MPa	Ratio of stress to Young's modulus, σ/E	Primary creep strain parameter, ϵ_p	Primary creep rate parameter, r, sec^{-1}	Minimum creep rate, $\dot{\epsilon}_{r1}$, sec^{-1}	Tertiary creep strain parameter, K	Tertiary creep rate parameter, s, sec^{-1}	Time to 1 percent strain, hr	Grain diameter, d, μm	Test duration	
		Time, hr	Temperature, °C											Time, hr	Strain, percent
B	S-74	0.33	1982	1316	103	6.30×10^{-4}	----------	----------	30.6×10^{-10}	1.76×10^{-2}	15.5×10^{-8}	829	81	1 466	2.19
	S-94	.5	1982	871	276	15.98	0.617×10^{-2}	0.048×10^{-6}	----------	----------	----------	--------	-----	23 694	.64
	S-90	↓	↓	1010	241	14.21	.546	.861	8.32	.447	10.5	1 800	86	4 324	2.40
	S-91			1066	207	12.25	.290	.861	7.35	3.31	1.83	2 640	96	6 385	2.11
	S-92			1121	172	10.28	.093	.827	3.32	1.58	1.94	6 100	104	6 764	1.10
	S-85			1191	138	8.29	----------	----------	5.42	2.07	2.40	4 440	114	5 347	1.24
	S-76			1191	172	10.36	.138	7.17	35.4	4.93	6.14	705	88	4 963	[a]15.09
	S-120			1260	89.6	5.43	----------	----------	2.45	1.04	2.60	7 250	113	8 307	1.19
	S-86			1260	103	6.26	----------	----------	4.32	1.35	3.57	4 360	82	5 206	1.24
	S-123			1260	117	7.10	----------	----------	11.9	2.86	3.73	2 220	100	2 257	1.02
	S-77			1316	68.9	4.20	----------	----------	4.24	1.30	2.99	5 286	77	5 908	1.15
	S-113			1371	34.5	2.12	----------	----------	1.58	.540	2.61	11 200	125	13 032	1.28
	S-106			↓	41.4	2.54	----------	----------	----------	----------	----------	--------	130	2 971	[c]1.16
	S-112				48.3	2.97	----------	----------	4.56	.792	5.18	4 440	109	4 513	1.02
	S-95				55.2	3.39	----------	----------	7.80	1.06	8.39	2 260	114	3 962	2.38
	S-119			↓	68.9	4.24	----------	----------	15.3	.785	22.6	1 020	109	1 145	1.18
	S-78			1399	34.5	2.13	----------	----------	2.39	.423	6.10	5 600	79	6 210	1.21
	S-93			1482	20.7	1.29	----------	----------	5.66	.262	23.2	--------	136	4 364	[k]3.80
	S-96			1510	17.2	1.08	----------	----------	----------	----------	----------	--------	117	5 303	[j]3.55
	S-114			1593	6.89	.439	----------	----------	----------	----------	----------	--------	788	7 728	[j]1.05
	S-97	↓	↓	1593	10.3	.658	----------	----------	----------	----------	----------	--------	498	4 505	[j]4.92
	S-138	100	1649	1316	103	6.30	----------	----------	26.5	1.27	20.6	790	126	934	1.25
	S-176	100	1649	↓	↓	↓	----------	----------	32.7	1.83	17.1	718	125	1 104	1.78
	S-183	5	1899				----------	----------	33.0	1.93	14.3	850	163	1 945	[a]3.35
	S-194	24	1799	↓	↓	↓	----------	----------	29.4	3.42	11.0	637	173	2 057	[a]4.13
C	S-212	1	1538	1316	103	6.30×10^{-4}	----------	----------	305×10^{-10}	0.808×10^{-2}	313×10^{-8}	72	9	98	1.64
	S-175	↓	1649	↓	↓	↓	----------	----------	77.5	.580	110	250	12	291	1.25
	S-213		1760				----------	----------	26.3	.912	38.9	527	17	628	1.28
	S-214		1871				----------	----------	22.9	1.06	22.1	840	43	939	1.19
	S-215		1982	↓	↓	↓	----------	----------	24.9	2.80	8.37	1 030	121	1 197	1.19

[a]Portion of curve above 3 percent strain excluded from analysis.

[c]Curve not analyzed because of erratic behavior.

[j]Curve not analyzed because of excessive calculated grain growth.

[k]Portion of curve above 1300 hr excluded from analysis because of excessive calculated grain growth.

where $\dot{\epsilon}_m$ is the minimum creep rate.

Various power and exponential terms were studied to fit the data from those curves exhibiting only tertiary creep. Power terms were considered unsuitable because of the complexity introduced by the use of multiple power terms. An exponential term was developed that provided better fit to the tertiary curves over a wider range of creep strain than that provided by any single power term. This relation is

$$\epsilon = \epsilon_0 + K(e^{st} - 1) \tag{3}$$

where K is the tertiary creep strain parameter and s is the tertiary creep rate parameter. Although the strain parameter ϵ_p in the primary creep term has physical meaning (ϵ_p is the total primary strain), no corollary physical significance is presently apparent for K. It was observed, however, that K decreased with increasing curvature of the strain-time plots. The excellent fit of this relation to creep curves exhibiting entirely tertiary creep is shown in figure 3.

Tertiary creep is frequently quite pronounced at very low strains, less than 0.5 percent. The degree of acceleration at these low strains strongly suggests that creep acceleration (at least in niobium and tantalum alloys) is largely an intrinsic structural phenomenon rather than primarily the result of an extrinsic factor such as local specimen necking.

The tertiary creep observed here is true tertiary as opposed to the inverted or sigmoidal types of primary creep that have been observed in other materials (ref. 16). This is shown by figure 4, where several creep curves are seen to continue the accelerating creep to strains as large as 7 to 15 percent.

The tertiary creep term can be combined with the primary creep term to give a general equation

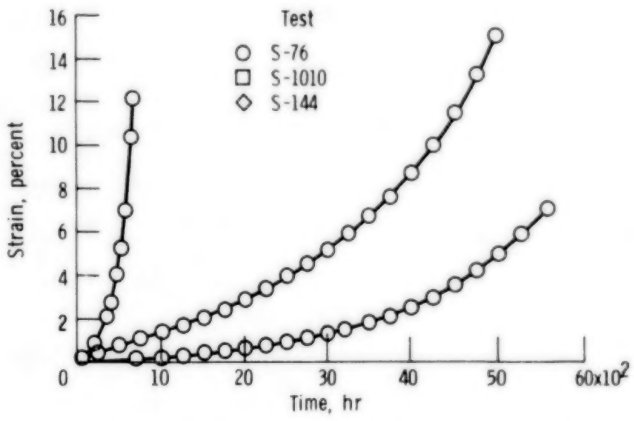

Figure 4. - Typical extended-strain creep curves, illustrating the continuous nature of tertiary creep.

describing creep curves consisting of both primary and tertiary creep:

$$\epsilon = \epsilon_0 + \epsilon_p(1 - e^{-rt}) + K(e^{st} - 1) \tag{4}$$

Figure 2 shows creep data fitted by equation (4).

A computer program was designed to analyze the creep curves generated during this study. This program contained options to allow nonlinear regression fitting of strain-time data from each creep test to any of the four relations represented by equations (1) to (4). Values of the appropriate coefficients for each creep curve were calculated and are given in table II, along with other pertinent test data.

The form of the creep rate-time curve is also of interest. The creep rate as a function of time is obtained by differentiating equation (4) as

$$\dot{\epsilon} = \epsilon_p r\, e^{-rt} + Ks\, e^{st} \tag{5}$$

The initial primary creep rate (at zero time) is equal to $\epsilon_p r$ and the initial tertiary creep rate is equal to Ks. (The minimum creep rate can be determined by differentiating equation (5), solving for the time when $d\dot{\epsilon}/dt$ equals zero, and then solving equation (4) for the creep rate at that time.) Creep rates calculated by linear regression over a number of short segments of two tests that exhibit primary and tertiary creep are shown in figure 5 to be well fitted by equation (5). Murphy and Uhrig (quoted by Conway and Flagella, ref. 8) also have shown that the creep rates for unalloyed tantalum can be correlated with time in the same manner as indicated by equation (5).

Equations (4) and (5) have significant implications, especially if they should prove widely applicable. These relations imply that creep can be considered as the sum of two separate but concurrent reactions, one decelerating with time and one accelerating with time. Both occur at finite rates at the initiation of creep. In this context "linear" creep is seen as the gradual transition between primary and tertiary creep. Linear creep can appear as a separate stage because the creep rate may change slowly during this transition. Although identification of these two reactions was beyond the scope of the present study, it is known that primary creep (decelerating creep rate) usually involves changes in the dislocation and/or subgrain arrangements into a more creep-resistant substructure (refs. 11 and 17). Tertiary creep (accelerating creep rate), on the other hand, is related to weakening by processes that include grain-boundary void nucleation and/or growth (ref. 18).

These weakening processes can begin as early as the start of a creep test, as shown by Boettner and Robertson (ref. 19) for void formation in copper.

Correlation of Tertiary Creep

In determining the stress and temperature dependency for tertiary creep (which constitutes the main portion of most of the creep curves), the initial tertiary creep rate Ks was used rather than the creep rate parameter s.

Analyses of the relation between creep rate and stress for coarse-grained (annealed 0.5 hr at 1982° C) and fine-grained (annealed 1 hr at 1649° C) materials indicated that the creep rate Ks for both materials exhibited a power dependency on stress at σ/E ratios below about 3×10^{-4} and an exponential dependency above this σ/E ratio. The sinh function (ref. 20) was used to incorporate both these stress dependencies into a single term:

$$Ks = A\left(\sinh \frac{\alpha\sigma}{E}\right)^n \tag{6}$$

where α is a stress factor related to both the exponential and power factors. Data for those lot A specimens annealed 0.5 hr at 1928° C are plotted according to equation (6) in figure 6. The preliminary stress-term exponents were 2.88 for these coarse-grained specimens and 2.23 for the fine-grained material. The stress factor α was essentially the same for both grain sizes.

The relation between the creep rate Ks and temperature is also complicated, with a change in temperature dependency at about 1130° C (0.43 Tm). This change in temperature dependency may be due to the creep reaction being related to lattice diffusion above 1130° C and to short-circuit diffusion along dislocations below 1130° C (ref. 21). However, the temperature dependencies were similar for the coarse- and fine-grained materials, suggesting no change in the basic rate-controlling deformation mechanisms with grain size. The change in temperature dependency with temperature was accommodated by a dual activation energy term given as

$$Ks = A\left(\sinh \frac{\alpha\sigma}{E}\right)^n \left(e^{-Q_1/RT} + c\, e^{-Q_2/RT}\right) \tag{7}$$

where A is a proportionality constant, Q_1 is the high-temperature activation energy, Q_2 is the low-temperature activation energy, and c is a dimensionless factor associated with the temperature of transition for Q_1 to Q_2. This treatment sums the different temperature dependencies of the two concurrent processes so that the effective temperature dependency reflects the separate contributions of each reaction at each temperature. The relation between (stress compensated) Ks and temperature for the fine- and coarse-grained materials is shown in figure 7. Values for Q_1, Q_2, and c were determined by simultaneous nonlinear regression analyses as 596 kJ/g mol, 319 kJ/g mol, and 3.89×10^{-11}, respectively, for both the coarse- and fine-grained materials. The apparent activation energy for creep at high temperatures (596 kJ/g mol) was higher than that for self-diffusion in tantalum, 413 kJ/g mol (ref. 22), and that for the diffusion of tungsten in tantalum, 498 kJ/g mol (ref. 23).

The effects of grain size on creep rate were evaluated on lots A, B, and C at 1316° C at stresses of 82.7 and 103 MPa. Creep curves for lot C at 103 MPa are shown in figure 8. Under these conditions the curves consist entirely of tertiary creep, with the creep rate being strongly affected by grain size. The initial tertiary creep rate Ks is shown as a function of grain size in figure 9. The rates decreased rapidly with increasing grain size at small grain sizes, less than about 50 μm, but tended to become constant at large grain sizes, greater than about 100 μm. This type of behavior has been observed for other tantalum-base alloys (ref. 1 and 3) and many other alloys (ref. 11). The increasing creep rates at large grain sizes reported by Shahanian and Lane for Monel (ref. 24) and by Garofalo, et al., for stainless steel (ref. 25) were not observed in the present study.

Analyses of the relation between the creep rate Ks and the grain size d at small grain sizes could not differentiate conclusively between $1/d^2$ and $1/d^3$, both of which have been proposed (refs. 26 and 27). However, the more generally accepted relation between creep rate and $1/d^2$ (ref. 11) appeared to fit the present data better and was used for all succeeding analyses.

In formulating a relation for expressing the creep rate Ks as a function of grain size, both intragranular and intergranular deformation must be considered. Based on the grain-size independence of creep in large-grained material, intragranular creep appears to predominate. The stress exponent near 3 for the coarse-grained material further suggests that dislocation glide inhibited by solute atmospheres is the rate-controlling reaction (ref. 11, 17, and 28). However, at fine grain sizes grain-boundary sliding becomes important. Accommodation of sliding by glide in the "mantle" regions adjacent to the grain boundaries may then control the creep rate, as suggested by Gifkins (ref. 29). The total creep rate is considered to be the sum of these two concurrent processes: glide, which is independent of grain size; and grain-boundary-sliding accommodation by glide

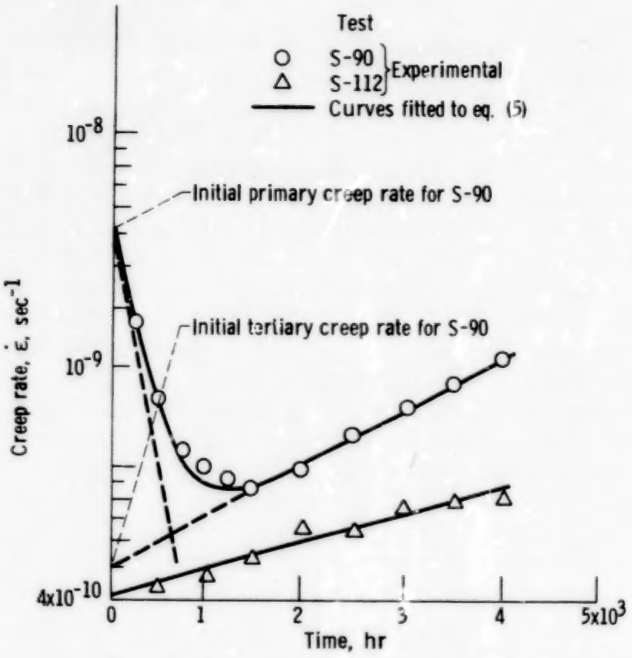

Figure 5. - Creep rate of Astar 811C as function of time for two tests.

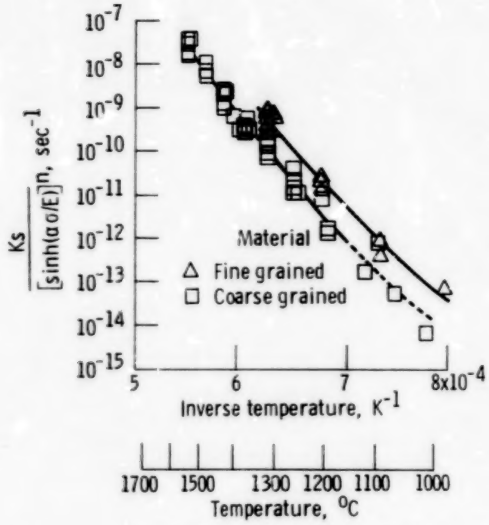

Figure 7. - Stress-compensated initial tertiary creep rate of Astar 811C as function of temperature.

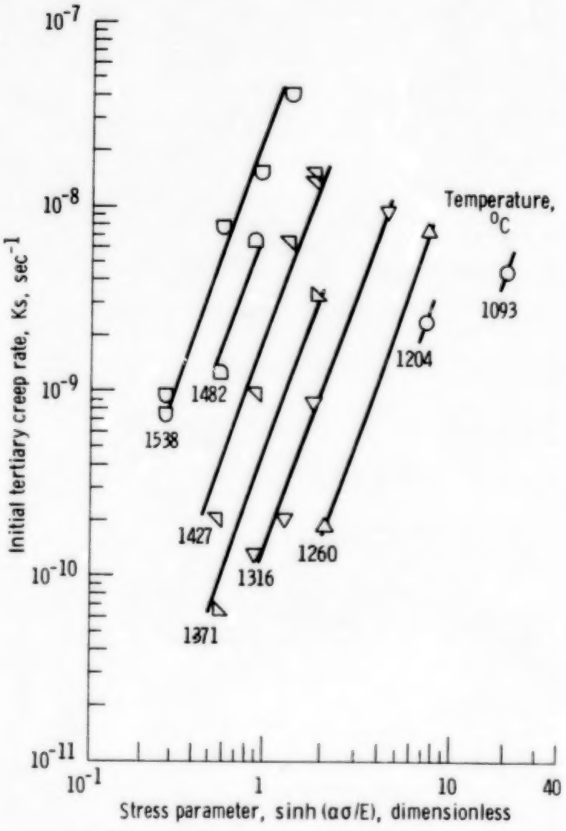

Figure 6. - Initial tertiary creep rate of Astar 811C as function of stress parameter for material lot A (annealed 0.5 hr at 1982^0 C). Slope of curves, 2.88.

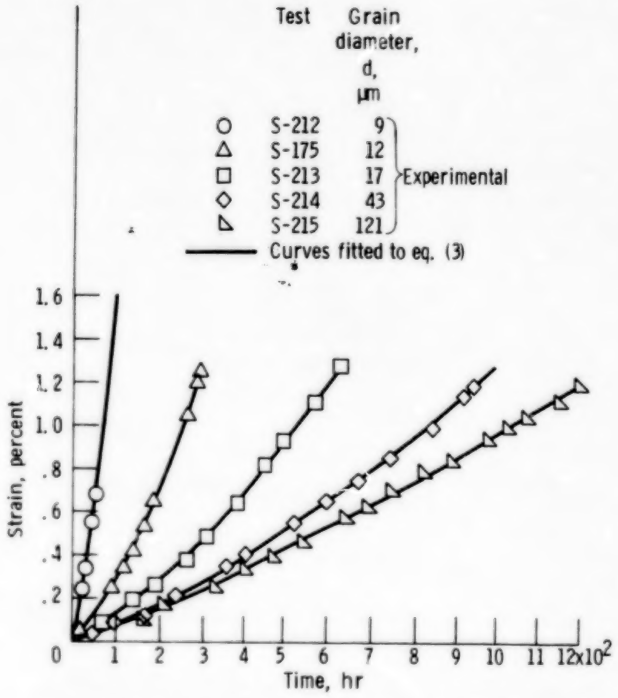

Figure 8. - Creep behavior of Astar 811C as function of grain size. All specimens from lot C; stress, 103 MPa; temperature, 1316^0 C.

in the grain mantle, which is approximately related to $1/d^2$.

The overall relation expressing the initial tertiary creep rate Ks as a function of stress, temperature, and grain size is

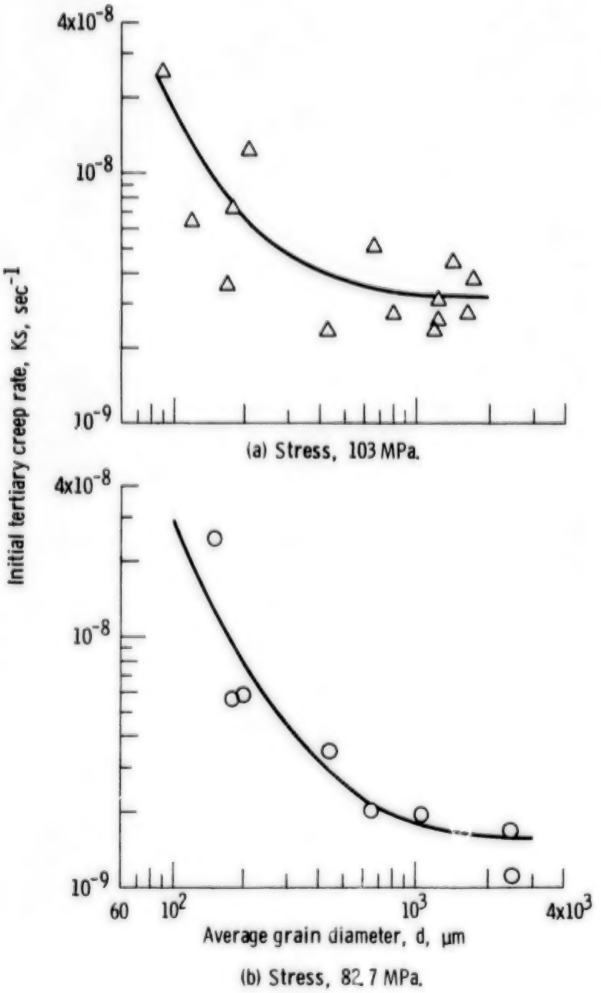

Figure 9. - Creep rate of Astar 811C as function of grain size. Temperature, 1316° C.

$$Ks = A\left[\left(\sinh\frac{\alpha\sigma}{E}\right)^{n_1} + \left(\frac{f}{d^2}\right)\left(\sinh\frac{\alpha\sigma}{E}\right)^{n_2}\right] \times \left(e^{-Q_1/RT} + c\,e^{-Q_2/RT}\right) \qquad (8)$$

where n_1 and n_2 are the stress-term exponents associated with intragranular deformation and intergranular-sliding-accomodation deformation, respectively, and f is a proportionality constant with dimensions of cm^2. At large grain sizes the first stress term predominates, but at small grain sizes the second stress term predominates. Figure 10 shows the temperature-compensated initial tertiary creep rate Ks as a function σ/E for the fine- and coarse-grained materials. Although the fine-grained material is significantly weaker than the coarse-grained material at low stresses, the strengths of the two materials are nearly equal at high stresses.

Design of two additional nonlinear regression computer programs was required to analyze the creep data according to equation (8). Values for the constants in equation (8) are summarized in table III. The value of 1.66 for n_2 is lower than the preliminary value of 2.23 previously calculated because the overall stress dependency in equation (8) is the sum of two terms rather than a single term as in equation (6).

Completion of the analysis of the tertiary creep behavior of Astar 811C required that the variables affecting the strain parameter K be determined. The parameter K was determined to be independent of temperature but varied with both stress and grain size. The relation between K and stress for the fine- and coarse-grained materials is shown in figure 11. Although considerable scatter exists in the data, a slope of unity gives a reasonable fit, suggesting a linear relation between K and σ/E.

It is also apparent from figure 11 that K is affected by grain size, since it is larger for coarse-grained material than for fine-grained material at the same value of σ/E. Although the nature of the variation of K with grain size cannot be determined from the present data, a power relation was assumed as a first approximation. Thus, K can be related to both stress and grain size by

$$K = A\left(\frac{\sigma}{E}\right)d^b \qquad (9)$$

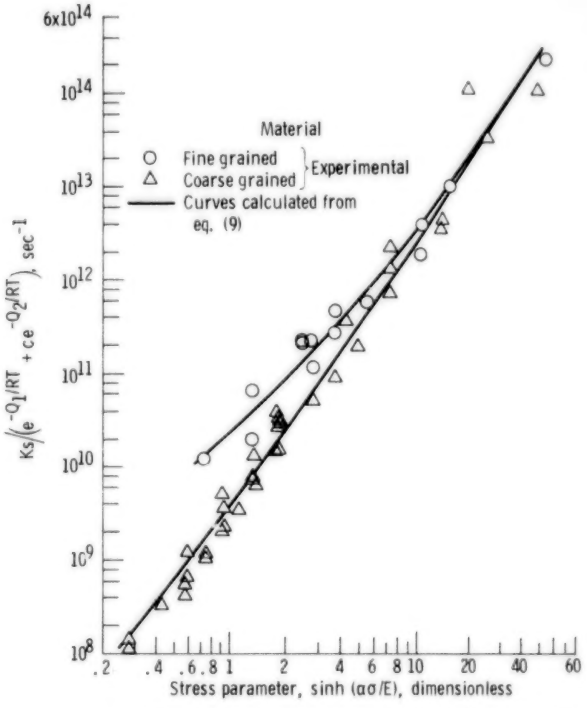

Figure 10. - Temperature-compensated initial tertiary creep rate of Astar 811C as function of stress parameter. Average grain diameter for coarse- and fine-grained materials, 104 and 17 μm, respectively.

TABLE III. - CREEP CONSTANTS FOR ASTAR 811C

Parameter	Equation			
	(8)	(10)	(13)	(14)
	Creep constants for indicated equations			
Proportionality constant, A, sec^{-1}	3.16×10^{9}	6.60×10^{10}	9.59×10^{8}	1.85×10^{12}
Stress factor, α	3220	----------	3180	4000
Exponential stress factor, β	----------	7220	---------	---------
Stress exponents:				
n_1	2.87	----------	2.77	2.23
n_2	1.66	----------	1.55	1.06
Grain-size factor, f, cm^2	1.85×10^{-5}	----------	1.47×10^{-5}	4.34×10^{-5}
Activation energy, kJ/g mol:				
Q_1	596	596	577	623
Q_2	319	319	345	387
Temperature factor, c	3.89×10^{-11}	3.89×10^{-11}	3.08×10^{-9}	6.78×10^{-9}
Correlation coefficient, R^2	0.861	0.843	0.874	0.824

where b is the exponent relating K to grain size d. The plot of $K/(\sigma/E)$ as a function of d in figure 12 shows a slope b of 0.35. The proportionality constant A has a value of 1.31×10^2.

The tertiary creep rate parameter s is obtained by dividing Ks from equation (8) by K from equation (9).

Correlation of Primary Creep

The approach for correlating primary creep parameters with stress and temperature was similar to that used previously for the tertiary creep parameters. The initial primary creep rate $\epsilon_p r$ (primary creep rate at zero time, fig. 5) was used for these correlations. However, since primary creep was generally observed only at high stresses, the stress dependency of $\epsilon_p r$ was best described by the exponential relation rather than by the sinh relation used for Ks. Unfortunately, the paucity of data precluded an independent determination of the relation between $\epsilon_p r$ and temperature. Since primary and secondary creep normally exhibit the same temperature dependence (ref. 16), the temperature function determined above for Ks was used for $\epsilon_p r$. The relation expressing $\epsilon_p r$ as a function of stress and temperature is

$$\epsilon_p r = A\, e^{\beta(\sigma/E)}\left(e^{-Q_1/RT} + c\, e^{-Q_2/RT}\right) \tag{10}$$

where β is the exponential stress factor. Values for the constants in equation (10) are given in table III. Figure 13 shows the relation of the temperature-compensated initial primary creep rate to stress. No variation in $\epsilon_p r$ with grain size was observed.

The relation of the total primary creep strain ϵ_p to stress determined as a power function is shown in figure 14. The relation is expressed as

$$\epsilon_p = A\left(\frac{\sigma}{E}\right)^m \tag{11}$$

where A is 1.44×10^7 and m is 3.34. As for the initial primary creep rate, no grain-size effects were noted for ϵ_p. The strong power dependence of total primary creep strain on stress observed here for Astar 811C is quite different from the weak parabolic dependence observed by Garofalo, et al., for stainless steel at 704° C (ref. 15). However, Evans and Wilshire did note a strong dependence of ϵ_p on stress for iron at low stresses (ref. 30). Apparently the effect of stress on total primary creep strain varies considerably among different materials.

The primary creep rate parameter r is calculated by dividing $\epsilon_p r$ from equation (10) by ϵ_p from equation (11).

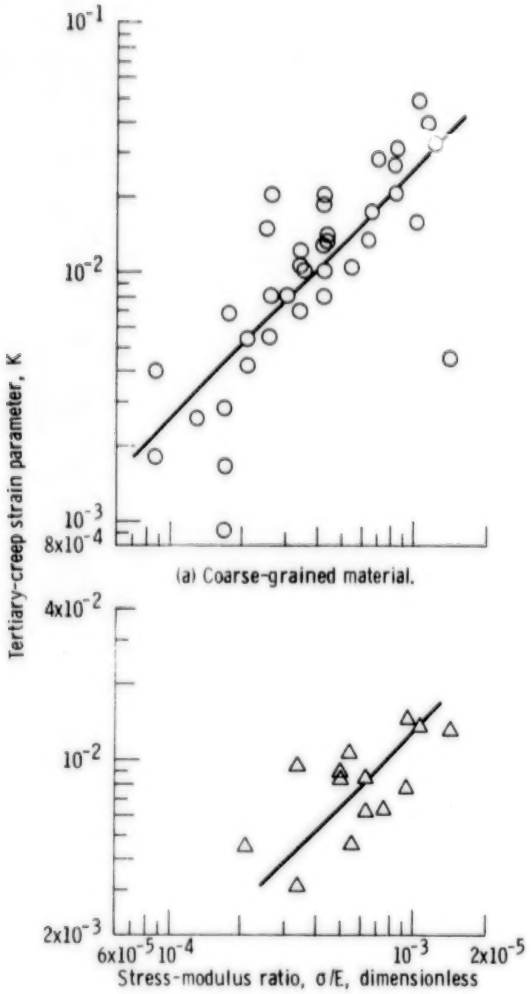

Figure 11. - Tertiary creep strain parameter of Astar 811C as function of stress-modulus ratio. Average grain diameters for coarse- and fine-grained materials, 104 and 17 μm, respectively.

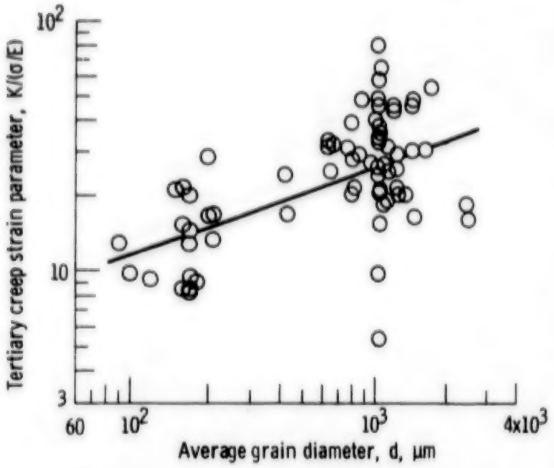

Figure 12. - Stress-compensated tertiary creep strain parameter of Astar 811C as function of grain size. Curve fitted by equation (9). Slope of curve, 0.35.

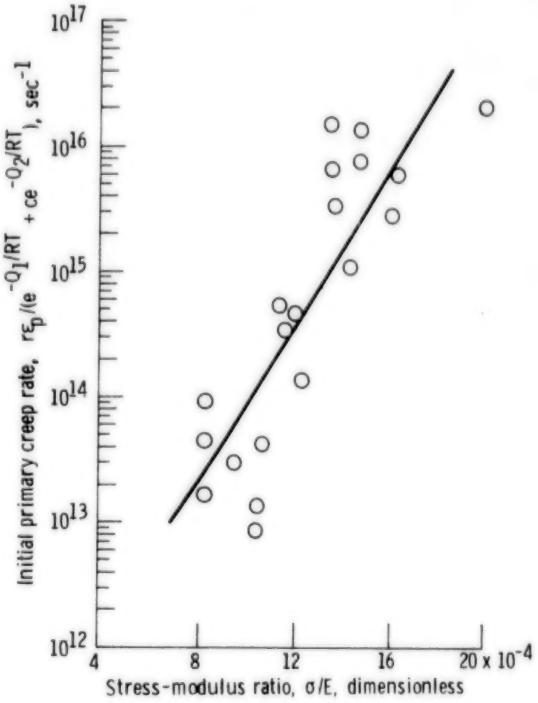

Figure 13. - Temperature-compensated initial primary creep rate of Astar 811C as function of stress-modulus ratio.

Anomalous Creep Behavior

During analyses of the creep curves it was observed that a minority of the creep curves exhibited deviations from the behaviors predicted by equations (1) to (4). These deviations were associated with either or both of two factors: excessive grain growth during creep testing, or excessive creep strain.

An example of anomalous behavior due to excessive grain growth is shown in figure 15. The creep curve from this 1538° C–6.89-MPa test initially exhibited tertiary creep similar to that shown by the low-stress tests in figure 3. However, after about 400 hr, the creep rate decreased until the test was terminated at 1455 hr. The decreasing creep rate after 400 hr is attributed to strengthening by grain coarsening. The average grain size of this specimen was 0.0112 cm after testing, as compared with 0.0017 cm for similarly annealed (1 hr at 1649° C) specimens tested at 1316° C or lower, an indication of substantial grain coarsening during testing.

Grain growth data from the various annealing treatments used in the present study were analyzed, as were grain growth data from several of the high-temperature creep tests. These data were correlated with time by a parabolic growth law:

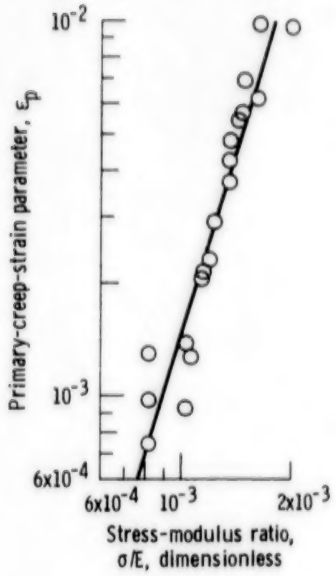

Figure 14. - Primary-creep strain parameters for Astar 811C as a function of stress-modulus ratio.

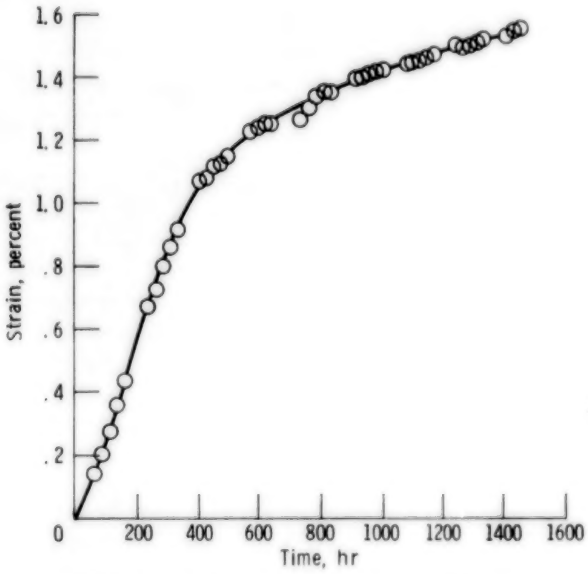

Figure 15. - Anomalous high-temperature creep curve, showing effects of grain coarsening during creep. Test S-180; stress, 6.89 MPa; temperature, 1538° C.

$$d^2 - d_0^2 = A t e^{-Q/RT} \qquad (12)$$

where d is the grain size at time t, d_0 is the initial grain size, A is a proportionality constant equal to 1.83×10^4 cm^2 sec^{-1}, Q is the apparent activation energy for grain growth, and T is the exposure temperature. An activation energy of 500 kJ/g mol was determined by linear regression analysis. This activation energy is close to the 498 kJ/g mol observed previously for diffusion of tungsten in tantalum (ref. 23) and suggests that the rate-controlling reaction for grain growth in Astar 811C is solute drag on the migrating boundaries (ref. 31). The relation between grain growth rate and temperature is illustrated in figure 16.

Consideration of the anomalous creep behavior caused by grain growth during testing indicated that a limit should be set on the creep data to be analyzed. On the basis of data fit to the expected creep relations, this limit was set as those time-temperature conditions that were calculated to cause a 50 percent increase from the initial grain size. Consequently those creep data beyond a calculated 50 percent increase in grain size were excluded from analysis, as indicated for several tests in table II. Analysis of a specimen with an initial grain size of 0.0117 cm would be limited to 2200 hr at 1300° C and 5 hr at 1600° C. Analysis of a specimen with a grain size of 104 μm would be limited to 83 000 and 140 hr, respectively, at the same temperatures. This limitation affects only the ability to analyze data from such specimens according to equations (1) to (4) and not the usefulness of such material in structural applications. Indeed, the alloy would be effectively strengthened by grain growth during service, as illustrated in figure 15.

In a similar manner creep data beyond a strain of 3 percent were excluded from analysis in order to

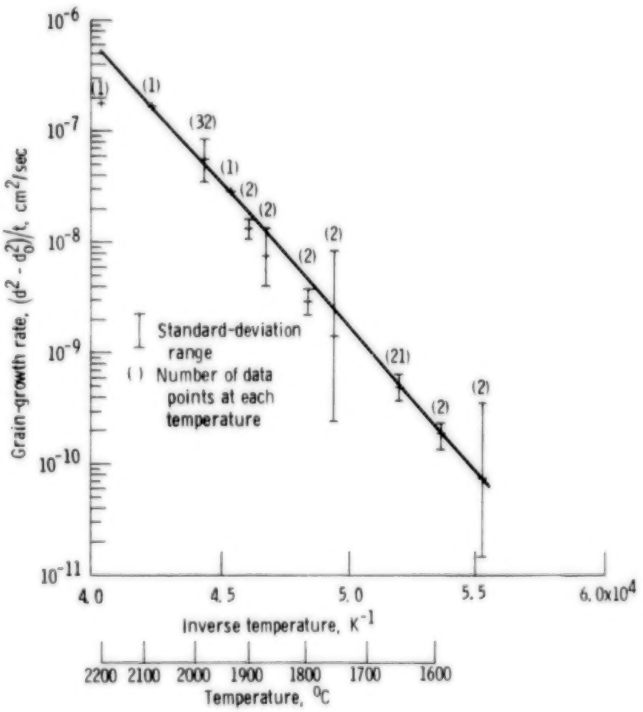

Figure 16. - Grain-growth rates as function of temperature.

eliminate anomalous behavior caused by reductions in the cross section and consequent increases in the effective creep stress.

Twenty-four of the 98 creep tests in this study were affected by these two limitations, with 10 being rejected because of calculated rapid grain growth. These affected tests are identified in table II.

Comparison of Calculated and Observed Creep Curves

We have now established relations for all the variables needed to calculate creep curves with equation (4) for all combinations of stress, temperature, and grain size covered by the present study. The primary creep parameters ϵ_p and r can be determined from equations (10) and (11); the tertiary creep parameters K and s can be determined from equations (8) and (9).

Calculated and observed creep curves are compared in figures 17 and 18. Periods of primary and tertiary creep are evident in figure 17. Good agreement between calculated and observed creep behavior was shown by tests at 179 and 200 MPa; fair agreement was shown by tests at 159 and 228 MPa. At a slightly higher temperature and lower stresses, only tertiary creep was observed (fig. 18). Here the differences in strength among lots A (tests N-2 and S-75), B (tests S-144 and S-101), and C (test S-175) are clearly evident. The calculated curves approximately average the divergent behaviors of the three lots.

The differences in creep strengths among lots A, B, and C are attributed to differences in rhenium content. Buckman and Goodspeed (ref. 32) have shown that the strength of Ta-W-Re-Hf alloys increases rapidly with increasing rhenium content. Thus lot B, with the highest rhenium content (table I), is stronger than lots A or C.

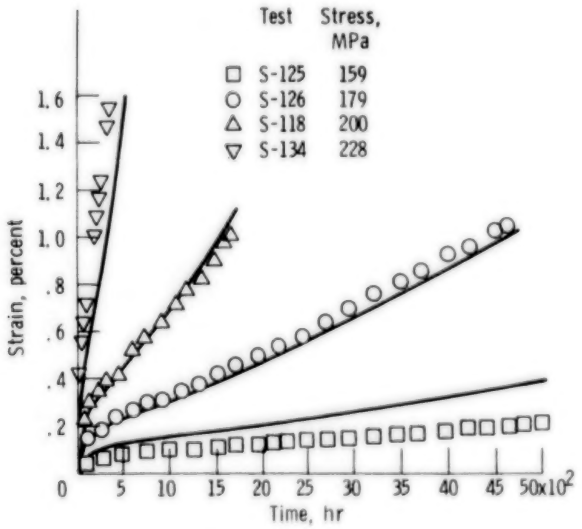

Figure 17. - Comparison of calculated creep curves for Astar 811C with experimental data points. All specimens annealed 1 hr at 1649° C and tested at 1093° C.

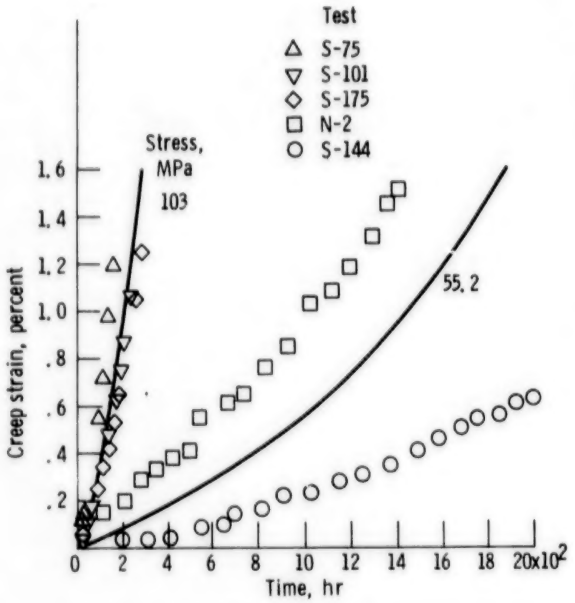

Figure 18. - Comparison of calculated creep curves for Astar 811C with experimental data points. All specimens annealed 1 hr at 1649° C and tested at 1316° C.

Examination of Creep-Tested Specimens

Oxygen analyses were performed on several Astar 811C specimens after creep testing in order to determine if the creep behavior of any particular specimen could have been affected by contamination. These analyses (table IV) indicate that most specimens underwent negligible changes in oxygen content during creep testing. Several specimens tested at 1482° and 1538° C did show moderate oxygen contamination, but this contamination had no apparent effect on creep behavior. Nitrogen analyses on selected specimens after creep testing revealed no significant increases in nitrogen content over that of the starting material. Potentially more serious were reductions of 50 to 75 percent in carbon content as a result of testing at 1538° C. However, these carbon losses also did not appear to change the creep behavior of the affected specimens.

Metallographic examination of annealed-plus-aged and of creep-tested specimens showed extensive carbide agglomeration at the grain boundaries but little or no intragranular precipitation. Figure 19 shows scanning electron micrographs of representative specimens. The grain-boundary carbide distribution is quite similar for aged (fig. 19(a)) and

TABLE IV. - ANALYSES OF CREEP-TESTED SPECIMENS

Test	Test temperature, °C	Test time, hr	Interstitial content after testing, ppm			Carbide
			O	N	C	
As received, lot A			13	18	250	-----
A	(a)	0	9	6	245	Ta_2C
B	(b)	0	20	7	248	Ta_2C
N-30	1093	479	10	--	---	-----
N-13	1093	[c]3 719	16	9	254	Ta_2C
N-27	1205	1 109	15	--	---	-----
N-35	1205	7 341	11	9	261	-----
N-26	1205	7 851	35	9	221	Ta_2C
N-29	1260	358	8	--	---	-----
N-33	1260	407	13	--	---	-----
N-4	1316	188	22	--	---	-----
N-36	↓	313	9	--	---	-----
N-5		361	5	--	---	-----
N-7		1 199	17	--	---	-----
N-6		1 440	15	--	---	-----
N-8		1 676	14	--	---	-----
N-2		1 843	62	--	---	-----
N-44		2 021	7	12	127	-----
N-1		[d]2 596	62	--	---	-----
N-28		2 925	4	7	234	Ta_2C
N-25		8 180	4	--	---	-----
N-21	↓	10 042	5	--	---	-----
N-18	1371	1 341	5	--	---	-----
N-23	1371	10 056	43	--	---	-----
N-15	1427	289	10	--	---	-----
N-14	↓	[e]865	38	--	---	-----
N-20		1 470	10	8	196	Ta_2C
N-10		[f]1 844	10	7	---	-----
N-22	↓	4 580	5	--	---	-----
N-31	1482	361	5	--	---	-----
N-19	1482	1 437	151	--	---	-----
N-11	1538	144	10	6	---	-----
N-24	↓	166	359	--	---	-----
N-16		315	9	10	97	Ta_2C
N-37	↓	514	385	16	52	-----

[a]Thermally exposed 0.5 hr at 1982° C plus 500 hr at 1205° C.

[b]Thermally exposed as identical to test A plus 500 hr at 1316° C.

[c]Creep tested for 2567 hr at 1093° C, 676 hr at 1205° C, plus 476 hr at 1316° C.

[d]Creep tested for 406 hr at 1316° C, 120 hr at 1288° C, 743 hr at 1260° C, 266 hr at 1232° C, plus 1061 hr at 1205° C.

[e]Creep tested for 263 hr at 1427° C, 192 hr at 1371° C, plus 410 hr at 1316° C.

[f]Creep tested for 524 hr at 1427° C plus 1320 hr at 1371° C.

creep-tested specimens (fig. 19(b)). No intergranular phase is discernible in specimen N-16 (fig. 19(c)), which lost most of its carbon during creep testing.

The grain-boundary particles were bromine-methanol extracted from five creep-tested specimens and two thermally aged specimens. Table IV gives the results of X-ray diffraction analyses on the extracted residues and shows that only the hexagonal-close-packed dimetal carbide Ta_2C was present, regardless of the prior thermal-mechanical treatment. No HfC was identifiable in the residues, although HfC might

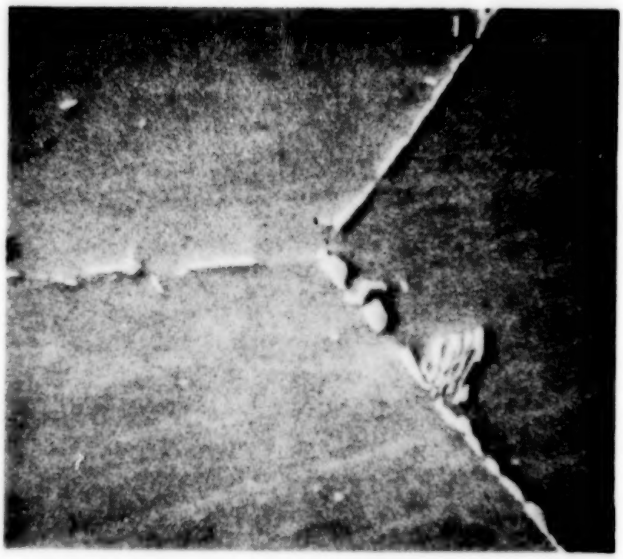

(a) Test B, heated for 0.5 hr at 1982° C, 500 hr at 1205° C, and 500 hr at 1316° C.

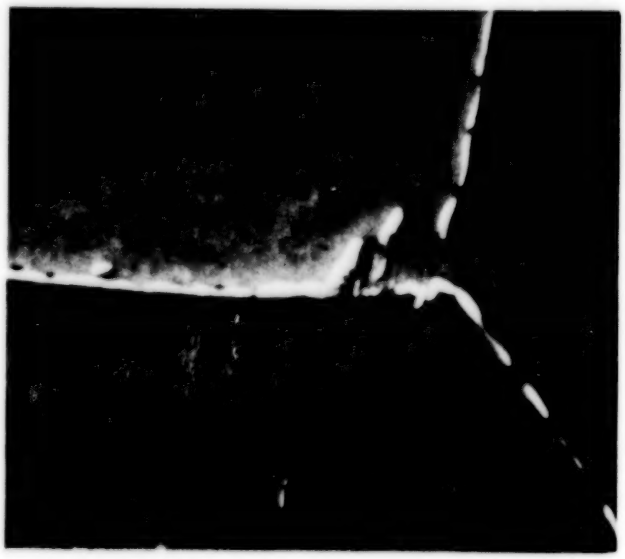

(b) Test N-28, creep tested for 2925 hr at 1316° C.

Figure 19. - Scanning electron micrographs of thermally exposed Astar 811C. X3000.

(c) Test N-16, creep tested for 315 hr at 1538° C.

Figure 19. Concluded.

be expected because of its high thermodynamic stability. These results are consistent with the observations of Buckman and Goodspeed (ref. 32), who also observed only Ta_2C in Astar 811C.

Although carbon contributes substantially to the creep strength of Astar 811C (ref. 32), the mechanism of strengthening is not well understood. It is obvious that coarse, intergranular carbide second phases such as those shown in figure 19 cannot be expected to strengthen by dislocation pinning, nor can carbon in solution be expected to inhibit dislocation mobility because of its high diffusivity. It is more probable that these carbides contribute to creep strength by inhibiting grain-boundary migration in the same manner that discontinuous grain-boundary carbides strengthen nickel-base superalloys (ref. 33).

Correlation of Minimum Creep Rate

Minimum creep rates were measured for all creep curves (except those exhibiting only primary creep) and are included in table II. These rates were analyzed by nonlinear regression as a function of stress, temperature, and grain size in the same manner as for the initial tertiary creep rate *Ks*. The relation for the minimum creep rate is

$$\dot{\epsilon}_m = A\left[\left(\sinh\frac{\alpha\sigma}{E}\right)^{n_1} + \left(\frac{f}{d^2}\right)\left(\sinh\frac{\alpha\sigma}{E}\right)^{n_2}\right] \times \left(e^{-Q_1/RT} + c\,e^{-Q_2/RT}\right) \qquad (13)$$

Values for the constants in equation (13) are given in table III. A plot of the temperature-compensated minimum creep rate as a function of stress is shown in figure 20 for both the fine- and coarse-grained materials.

Correlation of Time to 1 Percent Strain

The time-to-1-percent-strain parameter is frequently used for design purposes and can be correlated with stress, temperature, and grain size in the same manner as for the initial tertiary creep rate *Ks* and the minimum creep rate $\dot{\epsilon}_m$. The relation for t_{1pct} is

$$\frac{1}{t_{1pct}} = A\left[\left(\sinh\frac{\alpha\sigma}{E}\right)^{n_1} + \left(\frac{f}{d^2}\right)\left(\sinh\frac{\alpha\sigma}{E}\right)^{n_2}\right] \times \left(e^{-Q_1/RT} + c\,e^{-Q_2/RT}\right) \qquad (14)$$

Values for the constants in equation (14) are given in table III.

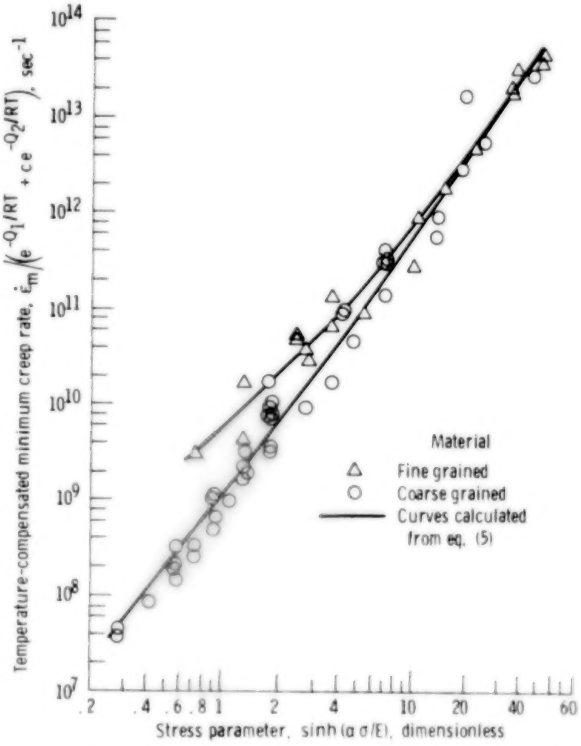

Figure 20. - Temperature-compensated minimum creep rate of Astar 811C as function of stress parameter. Average grain diameters for coarse- and fine-grained materials, 104 and 17 μm, respectively.

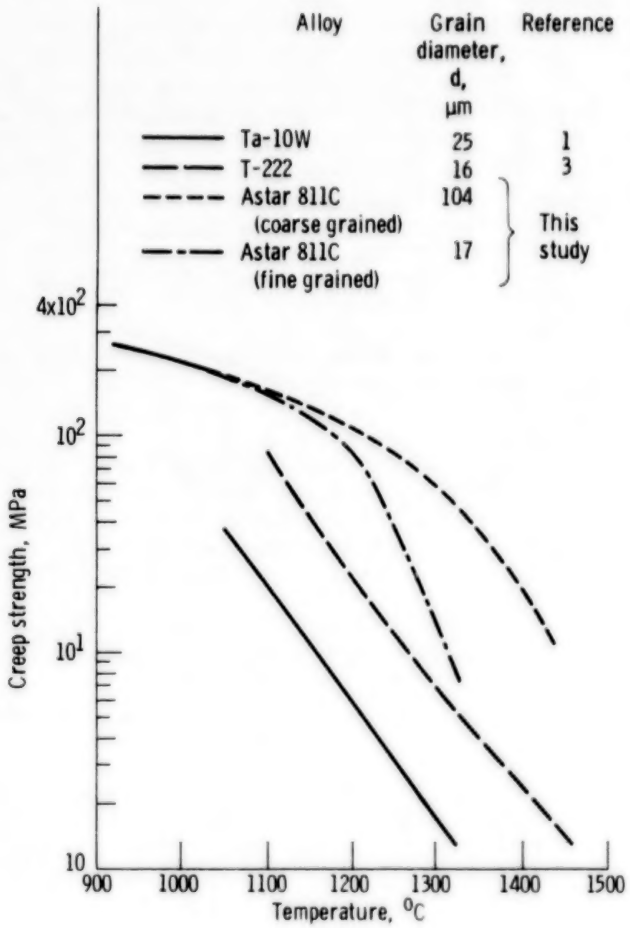

Figure 21. - Creep strength for 1 percent strain in 10 000 hours for tantalum alloys.

Comparison of Creep Strength of Astar 811C with Strengths of Other Tantalum Alloys

The creep strength for a strain of 1 percent in 10 000 hr is plotted as a function of temperature in figure 21 for fine-grained Ta-10W and T-222 (Ta-9.6W-2.4Hf-0.01C) (ref. 3) and for fine- and coarse-grained Astar 811C. The curves for Astar 811C were calculated from equation (4). At a stress of 30 MPa the fine-grained Astar 811C has approximately a 100 degree C use-temperature advantage over T-222, and the coarse-grained material has almost a 200 degree C advantage. The enhanced creep strength of Astar 811C over that of Ta-10W and T-222 is attributed primarily to solution strengthening by rhenium with a lesser contribution from grain-boundary pinning by carbon.

Conclusions

The following conclusions were drawn from this study of the long-time creep behavior of the tantalum alloy Astar 811C:

1. Astar 811C, like other tantalum and niobium alloys, exhibits primary creep at high stresses and low temperatures, tertiary creep at low stresses and high temperatures, and primary followed by tertiary creep at intermediate stresses and temperatures. No significant period of secondary creep is observed.

2. The creep curves for Astar 811C are well described by the Garofalo exponential term for primary creep plus a second exponential term for tertiary creep. The relation for the creep curve to strains of about 3 percent (in the absence of excessive grain growth) is given by

$$\epsilon = \epsilon_0 + \epsilon_p(1 - e^{-rt}) + K(e^{st} - 1)$$

where ϵ is total creep strain at time t, ϵ_0 is initial creep strain, ϵ_p is total primary creep strain, r is the primary creep rate parameter, K is the tertiary creep strain parameter, and s is the tertiary creep rate parameter.

3. The initial tertiary creep rate Ks can be related to stress by the sinh function. This rate can also be related to temperature by using an activation energy of 319 kJ/g mol below about 1130° C and an activation energy of 596 kJ/g mol above about 1130° C. The same temperature dependency can be used for the initial primary creep rate $\epsilon_p r$.

4. The primary creep strain parameter ϵ_p is a strong power function of stress but appears to be independent of grain size. However, the tertiary creep strain parameter K can be represented as a power function on both stress and grain size.

5. Coarse-grained material is significantly stronger than fine-grained material at low to intermediate stresses. The grain-size effect can be accommodated by expressing Ks as the sum of two stress terms, one related to the inverse square of grain size (predominate at small grain sizes) and one independent of grain size (predominate at large grain sizes). The stress exponents are 1.66 for the grain-size-dependent term and 2.87 for the grain-size-independent term. At high stresses, the creep strengths of the coarse- and fine-grained materials are nearly equal.

6. The stress exponent 2.87 for the coarse-grained material suggests that dislocation glide may be the rate-controlling creep reaction.

7. Correlation between calculated and observed creep curves ranged from good to fair. Differences between calculated and observed creep curves are

attributed to compositional differences among the three material lots studied.

8. The Astar 811C alloy has better long-time creep strength than the tantalum alloys Ta-10W, T-111, and T-222.

Lewis Research Center,
National Aeronautics and Administration,
Cleveland, Ohio, March 11, 1980,
506-16.

References

1. Titran, R.H.; and Klopp, W.D.: Long Time Creep Behavior of Tantalum-10 Tungsten in High Vacuum. NASA TN D-6044, 1970.

2. Sheffler, K.D.; Sawyer, J.C.; and Steigerwald, E.A.: Mechanical Behavior of Tantalum-Base T-111 Alloy at Elevated Temperature. Trans. ASMQ., vol. 62, no. 3, Sept. 1969, pp. 749-758.

3. Titran, R.H.: Creep Behavior of Tantalum Alloy T-222 at 1365 to 1700 K. NASA TN D-7673, 1974.

4. Titran, R.H.; and Hall, R.W.: High Temperature Creep Behavior of a Columbium Alloy, FS-85. NASA TN D-2885, 1965.

5. Hall, R.W.; and Titran, R.H.: Creep Properties of Columbium Alloys in Very High Vacuum. Refractory Metals and Alloys, III: Applied Aspects. R.I. Jaffee, ed., Gordon and Breach Science Publishers Inc., 1966, pp. 885-900.

6. Titran, R.H.; and Hall, R.W.: Ultrahigh-Vacuum Creep Behavior of Columbium and Tantalum Alloys at 2000° and 2200° F for Times Greater than 1000 Hours. Refractory Metals and Alloys, IV: Research and Development. R.I. Jaffee, G.M. Ault, J. Maltz, and M. Semchyshen, eds., Gordon and Breach Science Publishers Inc., 1967, pp. 761-774.

7. Klopp, W.D.; and Titran, R.H.: Interim Analysis of Long-Time Creep Behavior of Columbium C-103 Alloy. NASA TM X-71895, 1976.

8. Conway, J.B.; and Flagella, P.N.: Creep-Rupture Data for the Refractory Metals to High Temperatures. Gordon and Breach Science Publishers Inc., 1971, pp. 129-208.

9. Evans, W.J.; and Wilshire, B.: The High Temperature Creep and Fracture Behavior of 70-30 Alpha Brass. Metall. Trans., vol. 1, no. 8, Aug. 1970, pp. 2133-2139.

10. Wilshire, B.: Some Grain Size Effects in Creep and Fracture. Scr. Met., vol. 4, no. 5, 1970, 361-366.

11. Bird, J.E.; Mukherjee, A.K.; and Dorn, J.E.: Correlations Between High-Temperature Creep Behavior and Structure. UCRL-19056, California Univ., 1969. (CONF-690724-1)

12. Sawyer, J.C.; and Steigerwald, E.A.: Creep Properties of Refractory Metal Alloys in Ultra-High Vacuum. J. Mater., vol. 2, no. 2, June 1967, pp. 341-361.

13. Sherby, O.D.: Factors Affecting the High Temperature Strength of Polycrystalline Solids. Acta Met., vol. 10, no. 2, Feb. 1962, pp. 135-147.

14. Sheffler, K.D.; and Doble, G.S.: Influence of Creep Damage on the Low Cycle Thermal-Mechanical Fatigue Behavior of Two Tantalum-Base Alloys. (TRW-ER-7592, TRW Equipment Labs.; NASA Contract NAS3-13228.) NASA CR-121001, 1972.

15. Garofalo, F.; et al.: Strain-Time, Rate-Stress, and Rate-Temperature Relations During Large Deformations in Creep. Proceedings of Joint International Conference on Creep, Institution of Mech. Engineers, London, 1965, pp. 1-31 to 1-39.

16. Garofalo, F.: Fundamentals of Creep and Creep-Rupture in Metals. Macmillan Co., 1965, pp. 19-65.

17. Sherby, O.D.; and Burke, P.M.: Mechanical Behavior of Crystalline Solids at Elevated Temperature. Progress in Materials Science, Vol. 13, No. 7, B. Chalmers and W. Hume-Rothery, ed., Pergamon Press, Ltd. (Oxford), 1967, pp. 325-390.

18. Nemy, A.S.; and Rhines, F.N.: On the Origin of Tertiary Creep in an Aluminum Alloy. Trans. AIME, vol. 215, Dec. 1959, pp. 992-998.

19. Boettner, R.C.; and Robertson, W.D.: A Study of the Growth of Voids in Copper During the Creep Process by Measurement of the Accompanying Change in Density. Trans. AIME, vol. 221, June 1961, pp. 613-622.

20. Garofalo, F.: An Empirical Relation Defining the Stress Dependence of Minimum Creep Rate in Metals. Trans. AIME, vol. 227, Apr. 1963, pp. 351-356.

21. Robinson, S.L. and Sherby, O.D.: Mechanical Behavior of Polycrystalline Tungsten at Elevated Temperatures. Acta Met., vol. 17, Feb., 1969, pp. 109-125.

22. Pawel, R.E.; and Lundy, T.S.: The Diffusion of Nb95 and Ta182 in Tantalum. J. Phys. Chem. Solids, vol. 26, 1965, pp. 937-942.

23. Ivanov, A.N.; Krasilnikova, G.B.; and Mitin, B.S.: Determination of Diffusion Parameters in Molybdenum-Tantalum and Tungsten-Tantalum Systems. Fiz. Metal. Metalloved., vol. 29, no. 1, 1970, pp. 204-206.

24. Shahinian, P.; and Lane, J.R.: Influence of Grain Size on High Temperature Properties of Monel. Trans. ASM, vol. 45, 1953, pp. 177-199.

25. Garofalo, F.; Domis, W.F.; and von Gemmingen, F.: Effect of Grain Size on the Creep Behavior of an Austenitic Iron-Base Alloy. Trans. AIME, vol. 230, Oct. 1964, pp. 1460-1467.

26. Avery, D.H.; and Backofen, W.A.: A Structural Basis for Superplasticity. Trans. ASM, vol. 58, 1965, pp. 551-562.

27. Packer, C.M.; and Sherby, O.D.: An Interpretation of the Superplasticity Phenomenon in Two-Phase Alloys. Trans. ASMQ., vol. 66, no. 1, 1960, pp. 21-28.

28. Weertman, J.: Steady-State Creep of Crystals. J. Appl. Phys., vol. 28, no. 10, Oct. 1957, pp. 1185-1189.

29. Gifkins, R.C.: Grain-Boundary Sliding and Its Accommodation During Creep and Superplasticity. Metall. Trans., vol. 7A, no. 8, Aug. 1976, pp. 1225-1232.

30. Evans, W.J.; and Wilshire, B.: Transient and Steady-State Creep Behavior of Nickel, Zinc, and Iron. Trans. AIME, vol. 242, July 1968, pp. 1303-1307.

31. Aust, K. T.; and Rutter, J.W.: Grain Boundary Migration. Recovery and Recrystallization of Metals. L. Himmel, ed., Interscience Publishers, 1963, pp. 131-169.

32. Buckman, R.W., Jr.; and Goodspeed, R.C.: Considerations in the Development of Tantalum Alloys. Refractory Metal Alloys: Metallurgy and Technology. I. Machlin, R.T. Begley, and E.D. Weisert, eds., Plenum Press, 1968, pp. 373-394.

33. Sullivan, C.P.; and Donachie, M.J., Jr.: Some Effects of Microstructure on the Mechanical Properties of Nickel Base Superalloys. Met. Eng. Q., vol. 7, Feb. 1967, pp. 36-45.

1. Report No. NASA TP-1691	2. Government Accession No.	3. Recipient's Catalog No.
4. Title and Subtitle LONG-TIME CREEP BEHAVIOR OF THE TANTALUM ALLOY ASTAR 811C		5. Report Date September 1980 6. Performing Organization Code
7. Author(s) William D. Klopp, Robert H. Titran, and Keith D. Sheffler		8. Performing Organization Report No. E-041 10. Work Unit No. 506-16
9. Performing Organization Name and Address National Aeronautics and Space Administration Lewis Research Center Cleveland, Ohio 44135		11. Contract or Grant No. 13. Type of Report and Period Covered Technical Paper
12. Sponsoring Agency Name and Address National Aeronautics and Space Administration Washington, D.C. 20546		14. Sponsoring Agency Code

15. Supplementary Notes

William D. Klopp and Robert H. Titran, Lewis Research Center; Keith D. Sheffler, Pratt&Whitney Aircraft, East Hartford, Conn.

16. Abstract

The long-time, high-vacuum creep behavior of Astar 811C (Ta-8W-1Re-0.7Hf-0.025C) has been studied as a function of stress, temperature, and grain size. Primary creep strain was related to time by the Garofalo exponential function, and a second exponential term was developed to describe the tertiary portion of the creep curve. No significant periods of secondary (linear) creep were observed. The creep curves were well expressed by a relation that includes only terms for primary and tertiary creep: $\epsilon = \epsilon_0 + \epsilon_p (1 - e^{-rt}) + K(e^{st} - 1)$. The initial primary and tertiary creep rates $\epsilon_p r$ and Ks, obtained by differentiating the respective terms from the strain-time relation, can be related to temperature by using a dual activation energy to account for lattice and dislocation core diffusion. The term $\epsilon_p r$ is expressed as an exponential function of stress, and Ks can be related to stress by the sinh function. At small grain sizes, Ks is proportional to the inverse square of grain size. The strain parameters ϵ_p and K were determined as power functions of the applied stress. The overall relation for the initial tertiary creep rate Ks is $Ks = A\left[(\sinh \alpha\sigma/E)^{n_1} + (f/d^2)(\sinh \alpha\sigma/E)^{n_2}\right]\left(e^{-Q_1/RT} + c\,e^{-Q_2/RT}\right)$, where A is the proportionality constant, α is the stress factor, σ is the stress, E is Young's modulus, f is the grain-size factor, d is the grain size, n is the stress exponent, Q is the activation energy, R is the gas constant, T is the temperature, and c is the temperature factor. Similar relations were developed for the initial primary creep rate $\epsilon_p r$, the minimum creep rate $\dot{\epsilon}_m$, and the time to 1 percent strain.

17. Key Words (Suggested by Author(s))	18. Distribution Statement
Creep; Refractory metal; Tantalum; Astar 811C; Primary creep rate; Secondary creep rate; Tertiary creep rate; Temperature dependency; Stress dependency; Grain size; Activation energy	Unclassified - unlimited STAR Category 26

19. Security Classif. (of this report)	20. Security Classif. (of this page)	21. No. of Pages	22. Price*
Unclassified	Unclassified	20	A02

* For sale by the National Technical Information Service, Springfield, Virginia 22161

NASA-Langley, 1980